

# Multiple Equilibria in an Age-Structured Two-Sex Population Model

James D Montgomery  
Department of Sociology  
University of Wisconsin-Madison  
Madison, WI 53706  
jmontgom@ssc.wisc.edu

June 7, 2013

**Abstract** The complexity of age-structured two-sex population models has inhibited analysis of the uniqueness or stability of persistent distributions (i.e., equilibria in which the population grows exponentially with a fixed proportion in each age class). To offer some insight, this paper examines a special case in which couples dissolve only through the death of a spouse, and widows never remarry. Additional simplifying assumptions on the matching function (individuals meet through random mixing of the population; eligible singles have no age preference over potential partners) yield a tractable model in which equilibria are determined through a two-equation system that be studied graphically. For the exogenous-growth version of the model, we prove that multiple equilibria arise only if the population growth rate is negative. Numerical examples indicate that multiplicity also requires either a high matching rate or a large range of ages over which singles are eligible for matching. For the endogenous-growth version of the model, numerical examples demonstrate the potential for multiple equilibria, catastrophes, and limit cycles.

# 1 Introduction

While applied demographers work primarily with one-sex population models, many sociological applications require two-sex models that explicitly address matching of females and males into couples. Some important applications such as “marriage squeeze” (Schoen 1983, Guilmoto 2012) further require age-structured models that keep track of the age distributions of single females and single males as well as the joint distribution of ages across couples.

There is now a sizeable literature on two-sex population models both with and without age structures (e.g., Keyfitz 1972, Hoppensteadt 1975, Caswell and Weeks 1986, Pollak 1986, Schoen 1988, Hadelér 1989, Iannelli et al 2005). While standard models without an age structure seem to be well understood by mathematical demographers, much remains unknown about age-structured two-sex models. Several researchers have proven existence of persistent distributions given flexible specifications of the matching function (e.g., Prüss and Schappacher 1993, Martcheva 1999, Inaba 2000).<sup>1</sup> But the complexity of these models has precluded more exhaustive analysis addressing stability or uniqueness of these equilibria.

This complexity might prompt researchers to employ computational methods (see, e.g., Iannelli et al 2005, Ch 4), though the large number of parameters and initial conditions may still complicate efforts to fully characterize the behavior of these models. Thus, it remains useful for researchers to consider special cases that are more amenable to analysis and may provide insight into more general models. For example, by adding a maturation period to a model with no age structure, Hadelér (1993) developed a quasi-age-structured model and derived conditions under which it admits a unique non-trivial persistent distribution.

In this spirit, the present paper considers an age-structured two-sex model similar to one proposed by Inaba (1993) in which couples dissolve only through the death of a spouse, and widows never remarry. While a more realistic model would of course also permit divorce and remarriage, the sequential structure of an individual’s life-course (from single to married to widowed) simplifies analysis of the present model. Two further assumptions also greatly facilitate tractability. First, we adopt a particular specification of the matching function that presumes random mixing within the population. Second, we assume that singles match only within “eligible” age ranges, and that eligible singles have no age preference over potential partners. Given these simplifications, an equilibrium of the model is fully characterized by two variables – the population growth rate and the share of eligible females in the

---

<sup>1</sup>In the context of one-sex models, demographers commonly use the phrase “stable populations” rather than “persistent distributions” to refer to populations growing exponentially with a fixed proportion in each age class. Given the non-linearity of two-sex models, the latter phrase is adopted to acknowledge that these equilibria may or may not be stable in the dynamical systems sense (i.e., the population may or may not return to a persistent distribution following a small perturbation). In contrast, the linearity of one-sex models ensures a unique equilibrium that is globally stable (i.e., the population converges to the stable population from any initial condition).

population – and the problem of finding persistent distributions is reduced to a two-equation system that can be studied using graphical methods.<sup>2</sup>

After formal specification of the model, our analysis proceeds in two steps. Following the analytic strategy adopted by Pollak (1986, 1990), we initially assume the population growth rate is exogenously given. In this case, an equilibrium requires consistency between the shares of eligible females and eligible males in the population. Formally, an exogenous-growth equilibrium may be viewed as the fixed point of a one-dimensional non-linear equation determining the share of eligible females (equation 37 below). We then consider the model when the population growth rate is endogenous. Beyond the consistency condition just described, an endogenous-growth equilibrium also requires that the number of children produced by couples is consistent with the growth rate. This gives rise to a second non-linear equation involving the growth rate and the share of eligible females (equation 51 below).<sup>3</sup>

Throughout our analysis, we focus especially on the existence of multiple equilibria. The potential for multiple equilibria in age-structured two-sex models is already well known (see Iannelli et al 2005, p 29, for an example based on a simple model proposed by Keyfitz 1972). Nevertheless, the existing literature seems to provide little indication of the conditions under which multiple equilibria arise. Given exogenous growth, we prove that multiple equilibria arise only if the growth rate is negative. Numerical examples indicate that multiplicity also requires a sufficiently high matching rate and a sufficiently large range of eligible ages. Given endogenous growth, numerical examples demonstrate that an equilibrium with a positive growth rate may be accompanied by equilibria with negative growth rates. Examples further demonstrate the potential for catastrophes and limit cycles. The practical importance of these findings and directions for future research are discussed in the conclusion.

## 2 Model

Our model is cast in discrete time to facilitate numerical computation, but specified so that the continuous-time analog is a limiting case. Dividing each year into  $H \geq 1$  periods of length  $h = 1/H$ , we can approximate the continuous-time model by setting  $H$  sufficiently large (bounded only by computational capacity). Given this

---

<sup>2</sup>While adopted for the sake of mathematical tractability, these assumptions might also be defended on substantive grounds. Bhrolcháin (2001) argues that individuals have more flexible age preferences over partners than usually assumed by sociologists or demographers, and suggests that matching between partners of different ages is largely determined by availability in the population. Inaba (1993) argues that, at least in Japan, most children are born to couples which constitute first marriages for both partners. In the present model, marriages between widows that do not produce children would be essentially irrelevant to the analysis.

<sup>3</sup>While the exogenous-growth model provides a useful stepping stone toward the endogenous-growth model, it may also be of independent interest. Schoen (1983) develops a similar model (albeit with a different specification of the matching function) to study marriage squeeze.

specification, an individual who is  $a$  years old has lived at least  $aH$  periods and at most  $(a+1)H-1$  periods. Further assuming that all individuals die before reaching  $\omega$  years, the set of age classes is given by

$$\mathcal{A} = \{0, 1, \dots, \omega H - 1\} \quad (1)$$

To simplify our discussion of the model below, an individual's "age" corresponds to the number of periods (not years) that he or she has lived.

The population is composed of never-married individuals ("singles"), couples, and widows. Thus, the size of the population in period  $t$  is given by

$$\begin{aligned} N(t) = & \sum_{i \in \mathcal{A}} F(i, t) + \sum_{j \in \mathcal{A}} M(j, t) + 2 \sum_{i \in \mathcal{A}} \sum_{j \in \mathcal{A}} C(i, j, t) \\ & + \sum_{i \in \mathcal{A}} W_F(i, t) + \sum_{j \in \mathcal{A}} W_M(j, t) \end{aligned} \quad (2)$$

where  $F(i, t)$  denotes the number of single females of age  $i$ ,  $M(j, t)$  denotes the number of single males of age  $j$ ,  $C(i, j, t)$  denotes the number of couples with a female of age  $i$  and male of age  $j$ ,  $W_F(i, t)$  denotes the number of widowed females of age  $i$ , and  $W_M(j, t)$  denotes the number of widowed males of age  $j$ .

Each period, some singles form couples. While mathematical demographers have suggested a wide variety of functional forms for the matching function (see Pollard 1997 for a review), there remains little consensus about the best specification (see Ianelli et al 2005 for a recent empirical comparison). In the present paper, we assume that the number of new couples of type  $ij$  formed during period  $t$  is given by

$$\Phi(i, j, t) = \frac{h \mu(i, j) F(i, t) M(j, t)}{N(t)} \quad (3)$$

where  $\mu(i, j)$  reflects the "force of attraction" between females of age  $i$  and males of age  $j$ . To motivate this specification, suppose that, with probability  $h\pi$  each period, each individual meets someone drawn randomly from the population. Conditional upon a meeting between a single female of age  $i$  and a single male of age  $j$ , the pair becomes matched with probability  $\tilde{\mu}(i, j)$ . Type  $ij$  pairs are thus matched at rate  $\mu(i, j) = \pi \tilde{\mu}(i, j)$ . Note that, because  $\mu(i, j)$  incorporates the meeting rate as well as the matching probability, this parameter may take values greater than one.

The population is also altered each period through births and deaths. We assume that the number of girls born during period  $t$  is given by

$$B(t) = \sum_{i \in \mathcal{A}} \sum_{j \in \mathcal{A}} h \beta(i, j) C(i, j, t) \quad (4)$$

where  $\beta(i, j)$  is the birth rate for couples of type  $ij$ . The number of boys born in period  $t$  is given by  $sB(t)$  where  $s$  is the sex ratio at birth. Letting  $\delta_F(i)$  denote

the death rate for females at age  $i$ , a female survives from age  $i$  to age  $i + 1$  with probability  $[1 - h\delta_F(i)]$ . Similarly, letting  $\delta_M(j)$  denote the death rate for males at age  $j$ , a male survives from age  $j$  to age  $j + 1$  with probability  $[1 - h\delta_M(j)]$ . Our assumption that no one reaches  $\omega$  years implies  $h\delta_F(\omega H - 1) = h\delta_M(\omega H - 1) = 1$ .

Given these assumptions on the matching, birth, and death processes, population dynamics are characterized by the following system of equations:

$$F(i + 1, t + 1) = [1 - h\delta_F(i)] \left[ F(i, t) - \sum_{j \in \mathcal{A}} \Phi(i, j, t) \right] \quad (5)$$

$$M(j + 1, t + 1) = [1 - h\delta_M(j)] \left[ M(j, t) - \sum_{i \in \mathcal{A}} \Phi(i, j, t) \right] \quad (6)$$

$$C(i + 1, j + 1, t + 1) = [1 - h\delta_F(i)] [1 - h\delta_M(j)] [C(i, j, t) + \Phi(i, j, t)] \quad (7)$$

$$W_F(i + 1, t + 1) = [1 - h\delta_F(i)] \left[ W_F(i, t) + \sum_{j \in \mathcal{A}} h\delta_M(j) [C(i, j, t) + \Phi(i, j, t)] \right] \quad (8)$$

$$W_M(j + 1, t + 1) = [1 - h\delta_M(j)] \left[ W_M(j, t) + \sum_{i \in \mathcal{A}} h\delta_F(i) [C(i, j, t) + \Phi(i, j, t)] \right] \quad (9)$$

$$F(0, t + 1) = B(t) \quad (10)$$

$$M(0, t + 1) = sB(t) \quad (11)$$

$$C(0, j, t + 1) = C(i, 0, t + 1) = 0 \quad (12)$$

$$W_F(0, t + 1) = W_M(0, t + 1) = 0 \quad (13)$$

Thus, for a given birth cohort, the number of singles falls each period as singles become married or die. Fixing the birth cohort of both spouses, the number of couples rises as singles become married, but falls as one (or both) spouses die. Finally, for a given birth cohort, the number of widows rises as spouses die but falls as widows themselves die. As already discussed in the introduction, we have simplified population dynamics by ignoring several complications – couples dissolve only through the death of a spouse, and widows never remarry.

Our analysis is also facilitated by several additional simplifying assumptions. First, we assume that the force of attraction is constant across all “eligible” singles. More

precisely, we assume that the matching function is given by

$$\mu(i, j) = \begin{cases} \mu & \text{if } i \in \mathcal{E}_F \text{ and } j \in \mathcal{E}_M \\ 0 & \text{otherwise} \end{cases} \quad (14)$$

where

$$\mathcal{E}_F = \{\alpha_F H, \dots, \gamma_F H - 1\} \quad \text{and} \quad \mathcal{E}_M = \{\alpha_M H, \dots, \gamma_M H - 1\} \quad (15)$$

Conceptually, single females become “eligible” for marriage when they reach  $\alpha_F$  years and remain eligible until they reach  $\gamma_F$  years, single males become eligible when they reach  $\alpha_M$  years and remain eligible until they reach  $\gamma_M$  years, and attraction between eligible singles is not influenced by their ages. To show the implications of this assumption, we first substitute (3) into (5) and (6) to obtain

$$F(i + 1, t + 1) = [1 - h\delta_F(i)] \left[ 1 - \sum_{j \in \mathcal{A}} \frac{h\mu(i, j)M(j, t)}{N(t)} \right] F(i, t) \quad (16)$$

$$M(j + 1, t + 1) = [1 - h\delta_M(i)] \left[ 1 - \sum_{i \in \mathcal{A}} \frac{h\mu(i, j)F(j, t)}{N(t)} \right] M(j, t) \quad (17)$$

Using equation (14), these equations become

$$F(i + 1, t + 1) = \begin{cases} [1 - h\delta_F(i)] [1 - h\mu\sigma_M(t)] F(i, t) & \text{if } i \in \mathcal{E}_F \\ [1 - h\delta_F(i)] F(i, t) & \text{otherwise} \end{cases} \quad (18)$$

where

$$\sigma_M(t) \equiv \frac{1}{N(t)} \sum_{j \in \mathcal{E}_M} M(j, t) \quad (19)$$

is the share of eligible males in the population in period  $t$ , and

$$M(j + 1, t + 1) = \begin{cases} [1 - h\delta_M(j)] [1 - h\mu\sigma_F(t)] M(j, t) & \text{if } j \in \mathcal{E}_M \\ [1 - h\delta_M(j)] M(j, t) & \text{otherwise} \end{cases} \quad (20)$$

where

$$\sigma_F(t) \equiv \frac{1}{N(t)} \sum_{i \in \mathcal{E}_F} F(i, t) \quad (21)$$

is the share of eligible females in the population in period  $t$ . In this way, equation (14) implies that dynamics of single females is governed by the share of eligible males in the population, while the dynamics of single males is governed by the share of eligible females in the population.

To further simplify our presentation, we also assume females live for exactly  $\omega_F$  years and males live for exactly  $\omega_M$  years. Formally, age classes are now given by

$$\mathcal{A}_F = \{0, \dots, \omega_F H - 1\} \quad \text{and} \quad \mathcal{A}_M = \{0, \dots, \omega_M H - 1\} \quad (22)$$

and mortality rates become

$$\begin{aligned}\delta_F(i) &= 0 \quad \text{for all } i < \omega_F H - 1 \\ \delta_M(j) &= 0 \quad \text{for all } j < \omega_M H - 1\end{aligned}\tag{23}$$

While it would be straightforward to incorporate arbitrary mortality patterns into the analysis below, this will have little impact on our results if most individuals survive beyond the ages at which matching and fertility occur (as usually observed nowadays in developed countries). We thus ignore early mortality to focus on the effects of other parameters.

### 3 Exogenous growth

We begin our analysis by decoupling the birth process from the matching process. That is, in place of equations (10) and (11), we assume throughout this section that the birth cohort evolves according to

$$F(0, t + 1) = (1 + hr) F(0, t)\tag{24}$$

$$M(0, t + 1) = (1 + hr) s F(0, t)\tag{25}$$

where  $r$  is the (exogenous) growth rate of the population. Once we have considered the potential for multiple equilibria for a given growth rate, we will recouple the birth process with the rest of the model in Section 4.

Having fixed the growth rate, we further consider equilibria with persistent distributions of singles, couples, and widows. In particular, this implies

$$F(i, t + 1) = (1 + hr) F(i, t)\tag{26}$$

$$M(j, t + 1) = (1 + hr) M(j, t)\tag{27}$$

for every age class  $i$  and  $j$ . Using equations (22-23) and (26-27), equations (18) and (20) can be rewritten as

$$F(i + 1, t) = \begin{cases} (1 + hr)^{-1} [1 - h\mu\sigma_M(t)] F(i, t) & \text{if } i \in \mathcal{E}_F \\ (1 + hr)^{-1} F(i, t) & \text{otherwise} \end{cases}\tag{28}$$

$$M(j + 1, t) = \begin{cases} (1 + hr)^{-1} [1 - h\mu\sigma_F(t)] M(j, t) & \text{if } i \in \mathcal{E}_M \\ (1 + hr)^{-1} M(j, t) & \text{otherwise} \end{cases}\tag{29}$$

Note that all time-indexed variables share the same time index  $t$ . Thus, restricting our attention to some particular period  $t$  (in which the population follows a stable growth path), we can simplify our notation by suppressing the time index. Normalizing the size of the birth cohort so that  $F(0) = 1$ , and making use of the recursive structure of these equations, we obtain

$$F(i) = (1 + hr)^{-i} (1 - h\mu\sigma_M)^{\psi_F(i)}\tag{30}$$

$$M(j) = s (1 + hr)^{-j} (1 - h\mu\sigma_F)^{\psi_M(j)}\tag{31}$$

where the exponent on the final term is given by

$$\psi_g(k) = \begin{cases} 0 & \text{for } k \in \{0, \dots, \alpha_g H - 1\} \\ k - \alpha_g H & \text{for } k \in \mathcal{E}_g \\ (\gamma_g - \alpha_g)H & \text{for } k \in \{\gamma_g H, \dots, \omega_g H - 1\} \end{cases} \quad \text{for } g \in \{F, M\} \quad (32)$$

Population shares of eligible females and males are thus given by

$$\sigma_F = \chi_F(\sigma_M) \equiv \frac{1}{N} \sum_{i \in \mathcal{E}_F} (1 + hr)^{-i} (1 - h\mu\sigma_M)^{i - \alpha_F H} \quad (33)$$

$$\sigma_M = \chi_M(\sigma_F) \equiv \frac{s}{N} \sum_{j \in \mathcal{E}_M} (1 + hr)^{-j} (1 - h\mu\sigma_F)^{j - \alpha_M H} \quad (34)$$

where population size is

$$N = \sum_{i \in \mathcal{A}_F} (1 + hr)^{-i} + s \sum_{j \in \mathcal{A}_M} (1 + hr)^{-j} \quad (35)$$

Equation (33) indicates that the share of eligible females depends on the share of eligible males, while equation (34) indicates that the share of eligible males depends on the share of eligible females. Formally, an equilibrium is a pair  $(\sigma_F^*, \sigma_M^*)$  such that

$$\sigma_F^* = \chi_F(\sigma_M^*) \quad \text{and} \quad \sigma_M^* = \chi_M(\sigma_F^*) \quad (36)$$

Equivalently, we are looking for a fixed point

$$\sigma_F^* = \chi_F(\chi_M(\sigma_F^*)) \quad (37)$$

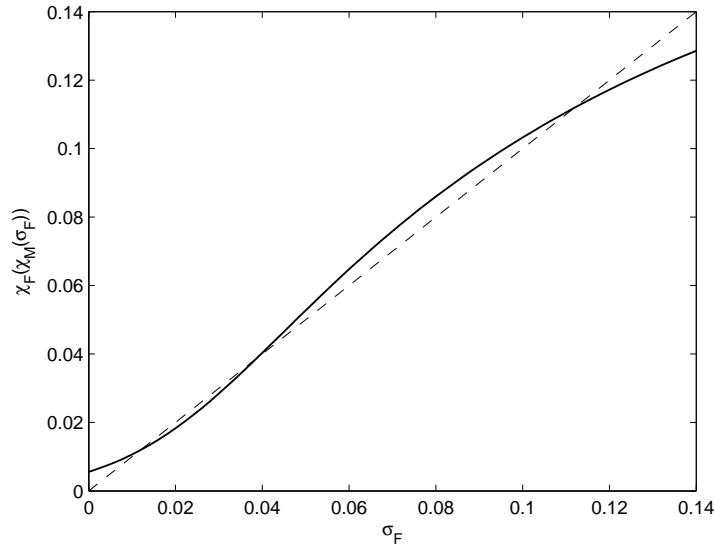
Because the distributions of singles are determined by the shares of eligible females and males (via equations 30 and 31), the distribution of couples is determined by the distributions of singles (via equation 7), and the distributions of widows are determined by the distribution of singles and couples (via equations 8 and 9), any solution to equation (37) fully determines the equilibrium. Having fixed the growth rate  $r$  (along with the other parameters  $\mu, s, \alpha_F, \alpha_M, \gamma_F, \gamma_M, \omega_F, \omega_M$ , and  $H = 1/h$ ), the problem of finding persistent distributions has thus been reduced to the problem of finding fixed points of a one-dimensional non-linear equation.

It is easy to establish the existence of at least one fixed point. Inspection of equations (33) and (34) reveals that  $\chi_F(\sigma)$  and  $\chi_M(\sigma)$  are continuous and decreasing in  $\sigma$  with  $1 > \chi_M(0) > \chi_M(1) > 0$  and  $1 > \chi_F(0) > \chi_F(1) > 0$ . Consequently, the compound function  $\chi_F(\chi_M(\sigma))$  is continuous and increasing in  $\sigma$  with

$$0 < \chi_F(\chi_M(0)) < \chi_F(\chi_M(1)) < 1 \quad (38)$$

Thus, there must be at least one fixed point  $\sigma_F^* \in [0, 1]$  satisfying equation (37). Perhaps the more interesting question is whether, for a given set of parameter values, there can be multiple equilibria.

**Figure 1: Plot of  $\chi_F(\chi_M(\sigma_F))$**



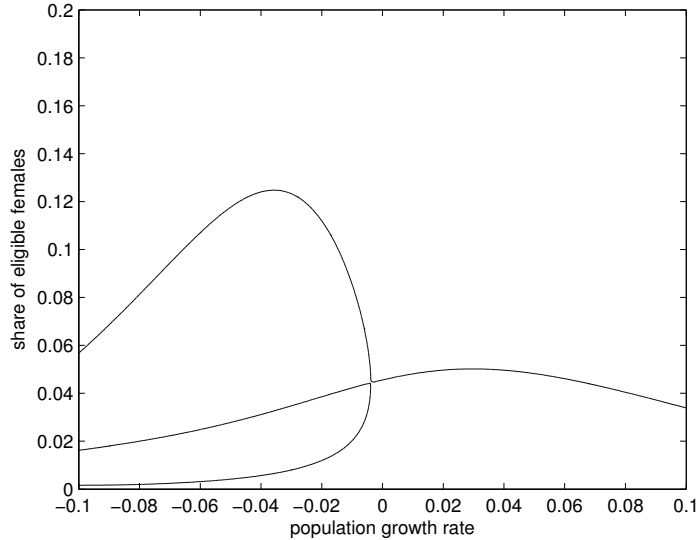
*This diagram plots the compound function  $\chi_F(\chi_M(\sigma_F))$  for parameter values  $r = -.02$ ,  $\mu = 3$ ,  $s = 1$ ,  $\alpha_F = \alpha_M = 20$ ,  $\gamma_F = \gamma_M = 60$ ,  $\omega_F = \omega_M = 80$ , and  $H = 1/h = 10$ . Solutions to equation (37) are indicated by the intersection of this function (solid curve) with the 45-degree line (dotted curve).*

To answer this question in the affirmative, we consider a numerical example. Setting the parameter values as indicated, Figure 1 plots the compound function  $\chi_F(\chi_M(\sigma_F))$  and reveals three different solutions to equation (37):  $\sigma_F^* = .012$ ,  $\sigma_F^* = .038$ , and  $\sigma_F^* = .112$ . The intermediate solution entails a symmetric equilibrium for males and females:  $\sigma_F^* = .038$  implies  $\sigma_M^* = \chi_M(.038) = .038$ . The other two solutions entail asymmetric mirror-image equilibria:  $\sigma_F^* = .012$  implies  $\sigma_M^* = \chi_M(.012) = .112$ , while  $\sigma_F^* = .112$  implies  $\sigma_M^* = \chi_M(.112) = .012$ .

It is important to recognize that Figure 1 establishes existence but not stability of equilibria. However, viewed naively as a cobweb diagram for a one-dimensional dynamical system (see, e.g., Allman and Rhodes 2004), Figure 1 suggests that  $\sigma_F$  would rise over time if  $\chi_F(\chi_M(\sigma_F)) > \sigma_F$  and fall over time if  $\chi_F(\chi_M(\sigma_F)) < \sigma_F$ . Hence, the equilibria at  $\sigma_F^* = .012$  and  $\sigma_F^* = .112$  would be stable while the equilibrium at  $\sigma_F^* = .038$  is unstable. Of course, the underlying dynamical system actually has many more dimensions. But simulation analysis indicates that, fixing a growth rate with multiple equilibria, the asymmetric equilibria are stable while the symmetric equilibria are unstable.<sup>4</sup>

<sup>4</sup>Given population dynamics determined by equations (5-9), (24-25), and (12-13), we computed trajectories for various initial conditions (distributions of singles, couples, and widows). An initial

**Figure 2: Exogenous growth equilibria**



*This diagram plots solutions to equation (37) for growth rates  $r \in [-.1, .1]$  holding fixed the other parameter values from Figure 1. It thus indicates the equilibrium value(s) of the share of eligible females  $\sigma_F^*$  for each exogenous growth rate  $r$ .*

Holding fixed the other parameter values from this numerical example, Figure 2 plots solutions to equation (37) for growth rates  $r$  ranging from  $-10\%$  to  $+10\%$ .<sup>5</sup> To reconcile Figure 2 with Figure 1, note that a growth rate of  $r = -.02$  generates the three equilibria already indicated. More generally, Figure 2 reveals the existence of three equilibria for a range of negative growth rates, but shows that there is a unique equilibrium for positive growth rates. For instance, a growth rate of  $r = .02$  generates a unique (and symmetric) equilibrium with  $\sigma_F^* = .050$  and  $\sigma_M^* = \chi_M(.050) = .050$ .

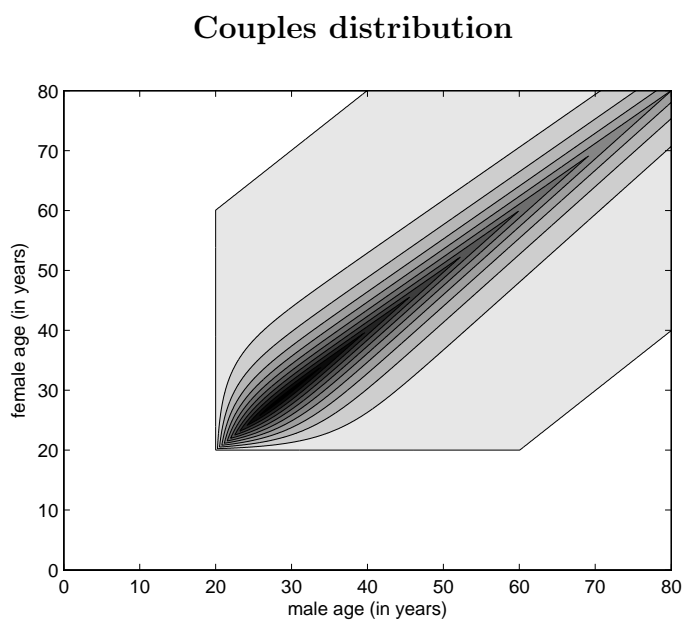
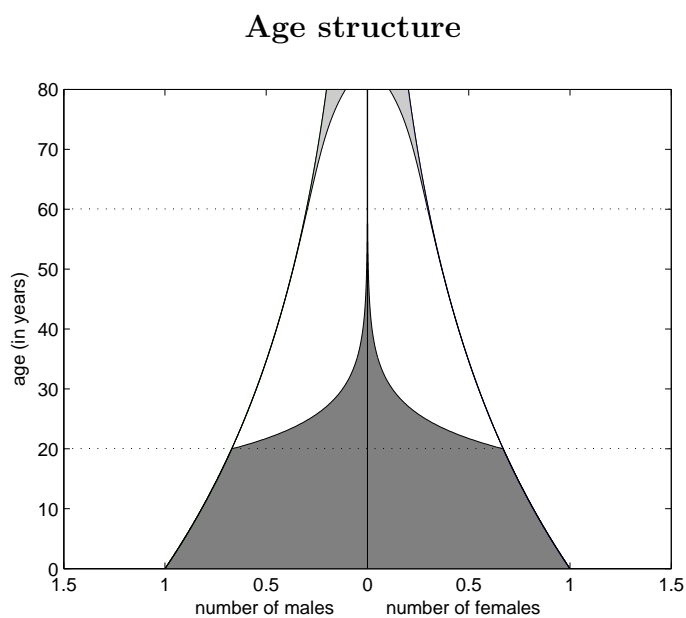
It may be instructive to consider the age structure and the distribution of couples implied in cases with positive and negative growth rates. Figure 3 illustrates the equilibrium outcomes when  $r = .02$ . The top panel shows the age structure, with singles in dark gray, members of couples in white, and widows in light gray. Note that the age pyramid becomes narrower at older ages, consistent with a growing population. The symmetry of the age structure follows from the symmetry of the equilibrium, as eligible females and males enter marriage at the same rate. The

---

condition in the neighborhood of one of the asymmetric equilibria converges to that equilibrium, but an initial condition in the neighborhood of the symmetric equilibrium diverges. When the initial condition is chosen arbitrarily, the population always converges to one of the asymmetric equilibria.

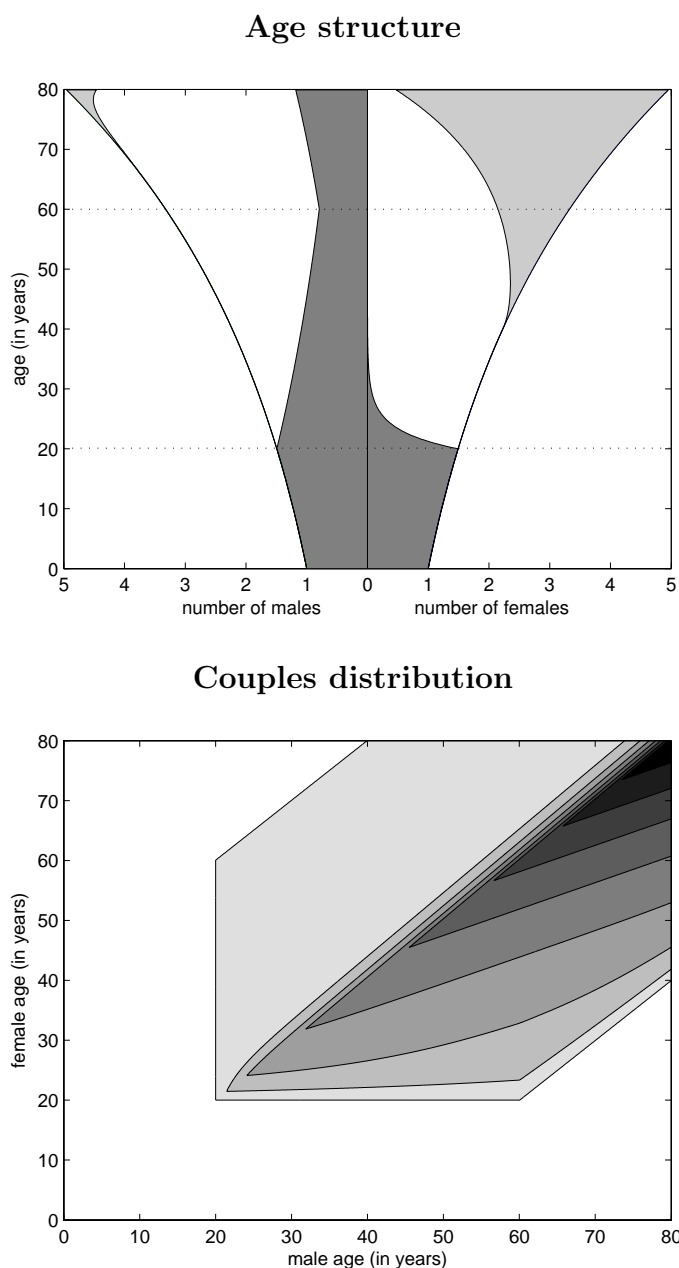
<sup>5</sup>We obtain this figure by evaluating the function  $\chi_F(\chi_M(\sigma_F)) - \sigma_F$  at every point on a fine grid in  $(r, \sigma_F)$  space, and then plotting the zero contour curve for the implied surface.

**Figure 3: Equilibrium population structure given  $r = .02$**



*These diagrams show the unique equilibrium population structure for  $r = .02$  given the other parameter values from Figure 1. The top panel depicts the age structure, with singles in dark gray, members of couples in white, and widows in light gray. The horizontal dotted lines indicate the range of eligibility for matching. The bottom panel depicts the distribution of couples, with darker shades of gray indicating higher densities.*

Figure 4: Equilibrium population structure given  $r = -.02$



*These diagrams show one of the asymmetric equilibrium population structures for  $r = -.02$  and the other parameter values from Figure 1. The top panel depicts the age structure, with singles in dark gray, members of couples in white, and widows in light gray. The horizontal dotted lines indicate the range of eligibility for matching. The bottom panel depicts the distribution of couples, with darker shades of gray indicating higher densities.*

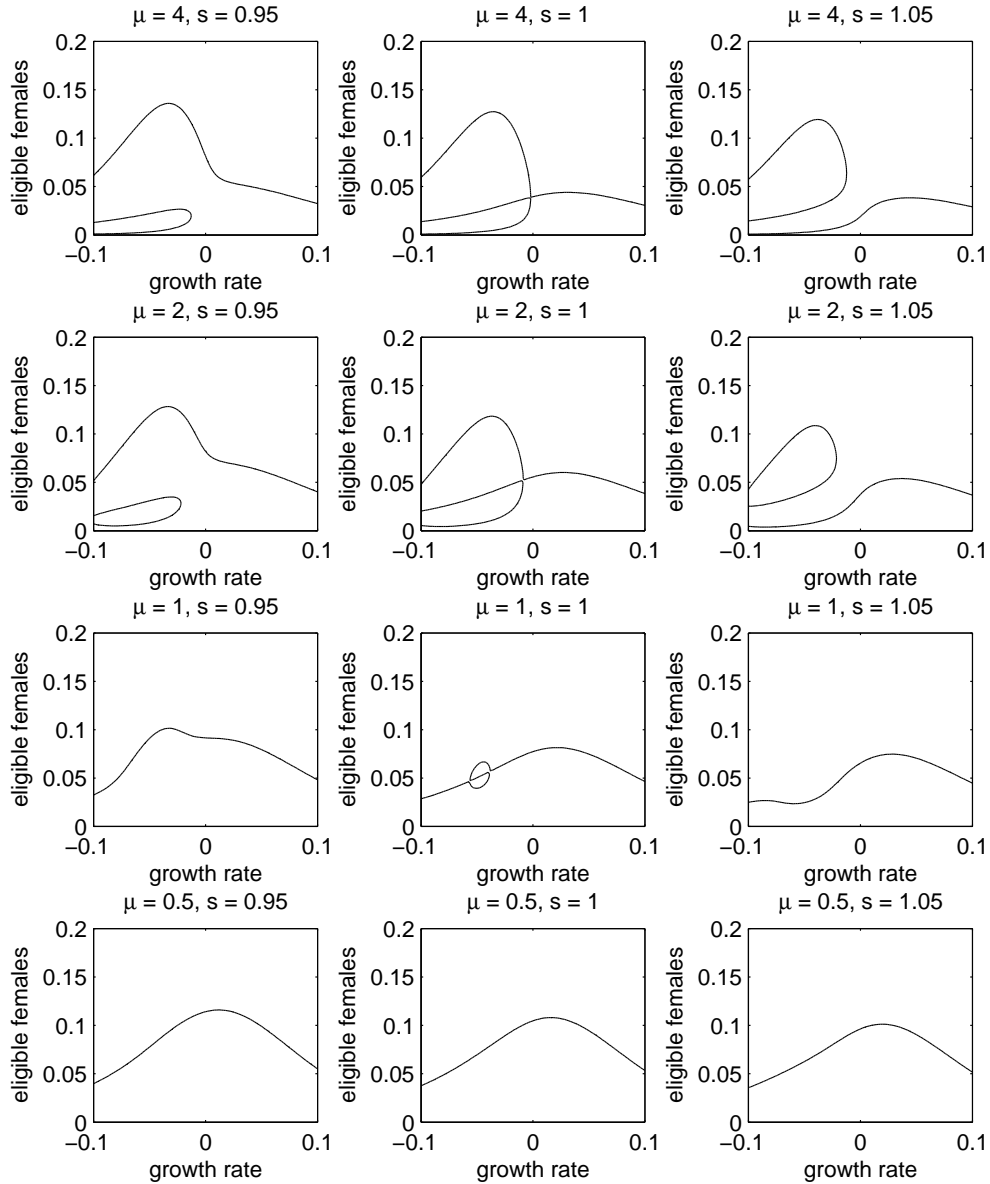
bottom panel gives a contour plot of the couples distribution, with darker shades of gray corresponding to higher densities. While our model presumes that the force of attraction is constant for all eligible pairs regardless of age, the equilibrium distribution of couples displays strong positive sorting by age. Intuitively, matching is driven by availability, and most eligible singles are young (as shown by the age distribution).

Figure 4 illustrates one of the (stable) asymmetric equilibrium outcomes when  $r = -.02$ . Note that the age pyramid becomes wider at older ages, consistent with a shrinking population. Given the asymmetry of this equilibrium ( $\sigma_F^* = .012$  and  $\sigma_M^* = .112$ ), the relatively large share of eligible males causes eligible females to quickly enter marriage. Conversely, the relatively small share of eligible females creates a backlog of eligible males. While the distribution of couples shows some positive sorting by age, the asymmetry of the age distribution of eligible singles induces asymmetry of the couples distribution, with husbands typically older than wives. Note also that the couples distribution is now skewed toward older couples, reflecting the negative growth rate of the population.

Figures 5 and 6 provide some sense of how the solutions of equation (37) vary with the parameters of the model. In Figure 5, we fix  $\alpha_F = \alpha_M = 20$ ,  $\gamma_F = \gamma_M = 60$ , and  $\omega_F = \omega_M = 80$ , and then consider  $\mu \in \{.5, 1, 2, 4\}$  and  $s \in \{.95, 1, 1.05\}$ . For each combination of parameters, the diagram gives the equilibrium share of eligible females  $\sigma_F^*$  for every growth rate  $r \in [-.1, .1]$ . The diagrams suggest that multiple equilibria arise when the matching rate  $\mu$  is sufficiently large, and the sex ratio at birth  $s$  is close enough to 1. In Figure 6, we repeat the same exercise, but with  $\gamma_F = \gamma_M = 50$  and  $\mu \in \{1, 2, 3, 4\}$ . Comparison of Figures 5 and 6 suggests that scope for multiple equilibria decreases as the range of eligible ages shrinks. Fixing the other parameters, additional examples (not reported) indicate that a matching rate of  $\mu \geq 5$  is needed to induce multiple equilibria when  $\gamma_F = \gamma_M = 45$ , and that a matching rate of  $\mu \geq 10$  is needed when  $\gamma_F = \gamma_M = 40$ .

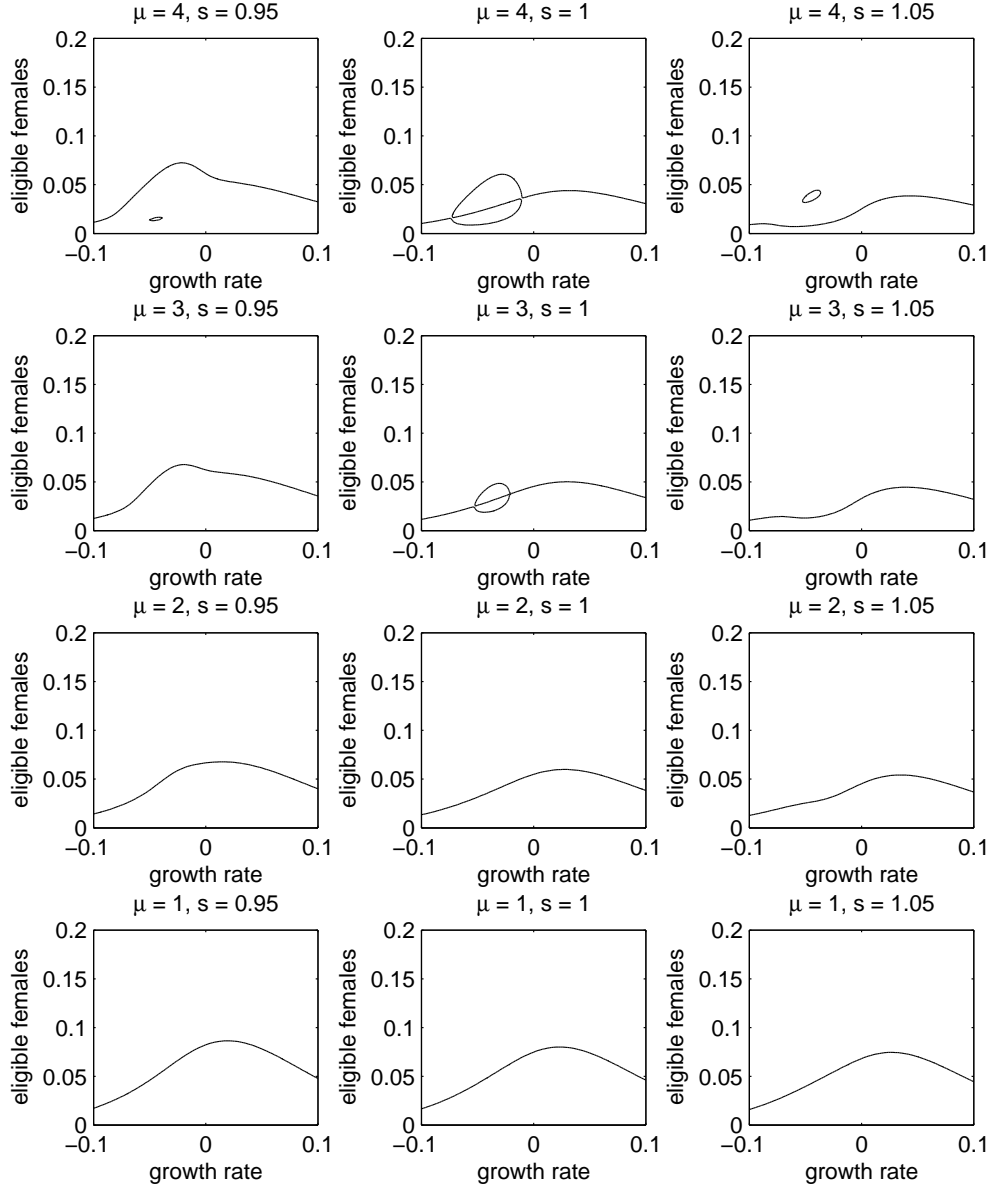
Perhaps the most interesting observation from Figures 5 and 6 is that multiple equilibria arise only when the growth rate is negative. This result also holds for additional examples (not reported) covering more of the parameter space and also permitting asymmetry between the sexes in the first age of eligibility ( $\alpha$ ), the last age of eligibility ( $\gamma$ ), and the age at death ( $\omega$ ). In the Appendix, using the continuous-time analogs of equations (33) and (34), we provide a formal proof that non-negative growth implies a unique equilibrium. Arguably, because populations with negative growth ultimately become extinct, this result might seem to undermine our emphasis on the potential for multiple equilibria. But as shown by Figures 5 and 6, multiple equilibria can arise even when the growth rate is only slightly below zero. Further, as we will see in the next section when we endogenize the growth rate, it may be possible (for a given set of parameter values) to have one equilibrium with a positive growth rate and other equilibria with negative growth rates.

Figure 5: Equilibrium outcomes given  $\gamma = 60$



Following the format of Figure 2, each diagram plots solutions to equation (37), indicating equilibrium value(s) of the share of eligible females  $\sigma_F^*$  for each exogenous growth rate  $r \in [-.1, .1]$ . The parameter values  $\alpha_F = \alpha_M = 20$ ,  $\gamma_F = \gamma_M = 60$ ,  $\omega_F = \omega_M = 80$ , and  $H = 1/h = 10$  are fixed across all diagrams. The matching rate  $\mu$  and the sex ratio at birth  $s$  vary across diagrams as indicated.

Figure 6: Equilibrium outcomes given  $\gamma = 50$



Following the format of Figure 2, each diagram plots solutions to equation (37), indicating equilibrium value(s) of the share of eligible females  $\sigma_F^*$  for each exogenous growth rate  $r \in [-.1, .1]$ . The parameter values  $\alpha_F = \alpha_M = 20$ ,  $\gamma_F = \gamma_M = 50$ ,  $\omega_F = \omega_M = 80$ , and  $H = 1/h = 10$  are fixed across all diagrams. The matching rate  $\mu$  and the sex ratio at birth  $s$  vary across diagrams as indicated.

## 4 Endogenous growth

We now consider the model with endogenous growth, replacing equations (24-25) with equations (10-11), so that population dynamics are given by equations (5-13).

In the absence of early mortality (equations 22-23), equation (7) becomes

$$C(i+1, j+1, t+1) = C(i, j, t) + \Phi(i, j, t) \quad (39)$$

Given the recursive structure of this equation, and the age ranges over which individuals may form couples (equation 15), we obtain

$$C(i, j, t) = \sum_{\tau=\underline{\tau}(i,j)}^{\bar{\tau}(i,j)} \Phi(i-\tau, j-\tau, t-\tau) \quad (40)$$

where

$$\underline{\tau}(i, j) = \max\{i - \gamma_F H + 1, j - \gamma_M H + 1, 1\} \quad (41)$$

$$\bar{\tau}(i, j) = \min\{i - \alpha_F H, j - \alpha_M H\} \quad (42)$$

Intuitively,  $\underline{\tau}(i, j)$  is the number of periods since an  $ij$  couple could have most recently formed, and  $\bar{\tau}(i, j)$  is the number of periods since an  $ij$  couple could have first formed. Note that  $\underline{\tau}(i, j) = 1$  if both the female and male are currently eligible for matching. If either the female or the male is not yet eligible, then  $\bar{\tau}(i, j) < 0$  and hence  $C(i, j, t) = 0$ .

We continue to consider equilibria with persistent distributions. Equation (40) may thus be written as

$$C(i, j) = \sum_{\tau=\underline{\tau}(i,j)}^{\bar{\tau}(i,j)} \Phi(i-\tau, j-\tau) (1+hr)^{-\tau} \quad (43)$$

where the time index  $t$  has been suppressed. Given our specification of the matching function (equations 3 and 14), and using equations (30-32) to determine  $F(i)$  and  $M(j)$ , we obtain

$$C(i, j) = \frac{sh\mu}{N} \sum_{\tau=\underline{\tau}(i,j)}^{\bar{\tau}(i,j)} (1+hr)^{-i-j+\tau} (1-h\mu\sigma_M)^{i-\tau-\alpha_F H} (1-h\mu\sigma_F)^{j-\tau-\alpha_M H} \quad (44)$$

where population size  $N$  is given by equation (35). Fixing the parameters of the model, each element of the couples distribution is thus determined by the growth rate  $r$ , the share of eligible females  $\sigma_F$ , and the share of eligible males  $\sigma_M$ .

Our specification of the birth process (equation 4) allows fertility rates to vary arbitrarily with the ages of the partners. But to reduce the number of fertility

parameters, it is convenient to assume that the fertility rate is constant for all couples within a fixed age range, and is zero otherwise. Under this assumption, the number of female births becomes

$$B = h \beta \sum_{i \in \mathcal{R}_F} \sum_{j \in \mathcal{R}_M} C(i, j) \quad (45)$$

where

$$\mathcal{R}_F = \{\alpha_F H, \dots, \kappa_F H - 1\} \quad (46)$$

$$\mathcal{R}_M = \{\alpha_M H, \dots, \kappa_M H - 1\} \quad (47)$$

are the fertile age ranges for females and males. Note that this specification permits asymmetry between females and males so that (for instance) couples with older males (but not older females) have positive fertility rates. Substituting equation (44) into equation (45), we can define

$$\rho(r, \sigma_F, \sigma_M) = \frac{sh^2 \beta \mu}{N} \sum_{i \in \mathcal{R}_F} \sum_{j \in \mathcal{R}_M} \sum_{\tau = \underline{\tau}(i, j)}^{\bar{\tau}(i, j)} (1+hr)^{-i-j+\tau} (1-h\mu\sigma_M)^{i-\tau-\alpha_F H} (1-h\mu\sigma_F)^{j-\tau-\alpha_M H} \quad (48)$$

which gives the number of female births as a function of the growth rate  $r$ , the share of eligible females  $\sigma_F$ , and the share of eligible males  $\sigma_M$ .

In equilibrium, the number of births must be consistent with the growth rate. Substituting equation (26) into equation (10), we obtain

$$(1+hr) F(0) = B \quad (49)$$

Because we have normalized  $F(0)$  to 1, the equilibrium condition is thus

$$1+hr^* = \rho(r^*, \sigma_F^*, \sigma_M^*) \quad (50)$$

From our analysis in the preceding section, equilibrium also requires consistency between the distribution of females and males, as stated in equation (36). An equilibrium of the endogenous-growth model is thus a triple  $(r^*, \alpha_F^*, \alpha_M^*)$  determined by the pair of equations (36) and equation (50). Equivalently, equilibrium is a pair  $(r^*, \alpha_F^*)$  determined by equation (37) and

$$1+hr^* = \rho(r^*, \sigma_F^*, \chi_M(\sigma_F^*)) \quad (51)$$

In this way, the problem of finding equilibria with persistent distributions has been reduced to the problem of solving a two-dimensional non-linear system.

Plotting solutions to equations (37) and (51), endogenous growth equilibria are determined by the intersections of these curves, as illustrated in Figure 7.<sup>6</sup> This

---

<sup>6</sup>To plot solutions to equation (51), we first evaluate the function  $\rho(r, \sigma_F, \chi_M(\sigma_F)) - (1+hr)$  at every point on a fine grid in  $(r, \sigma_F)$  space, and then plot the zero contour curve for the implied surface.

example retains the parameter assumptions from Figure 2, and makes the additional assumptions indicated. The thin curves indicate solutions to equation (37), and the thick curve indicates solutions to equation (51). Given  $\beta = .1$ , the top panel indicates a unique equilibrium ( $r^* = .009, \sigma_F^* = .048$ ). Simulation analysis (using population dynamics from equations 5-13) reveals that this equilibrium is stable. Given  $\beta = .08$ , the bottom panel indicates three different equilibria: ( $r^* = .001, \sigma_F^* = .046$ ), ( $r^* = -.006, \sigma_F^* = .068$ ), and ( $r^* = -.051, \sigma_F^* = .117$ ). Simulation analysis reveals that the equilibria with the highest and lowest growth rates are stable, while the equilibrium with the intermediate growth rate is unstable.

It is straightforward to consider graphically the effect of a change in the fertility rate  $\beta$ . To obtain the thick curve (representing solutions to equation 51), we plotted the zero contour lines for the function

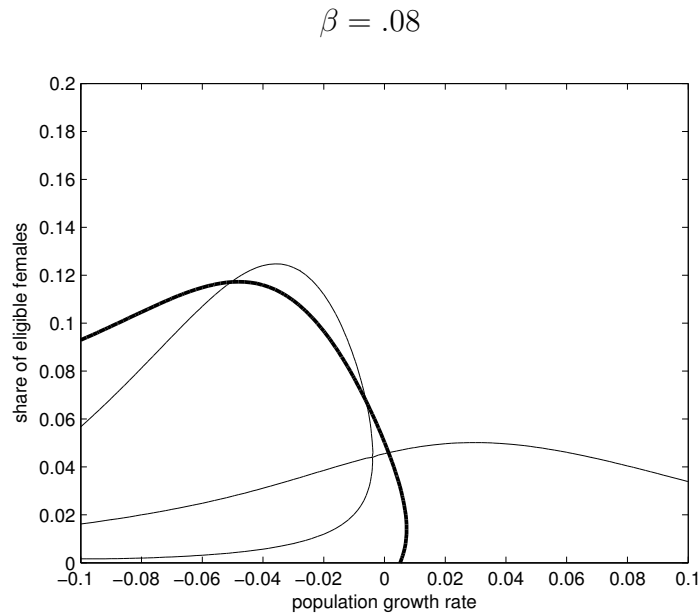
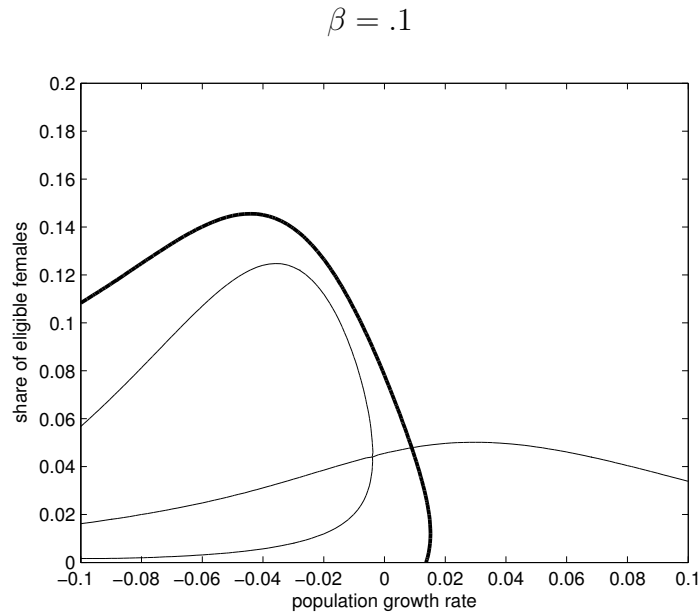
$$\rho(r, \sigma_F, \chi_M(\sigma_F)) - (1 + hr) \quad (52)$$

This function is positive in the region bounded by the thick curve (at the lower left of the diagrams in Figure 7) and negative outside of this region. Inspection of equation (48) reveals that  $\rho(r, \sigma_F, \chi_M(\sigma_F))$  is increasing in the fertility rate  $\beta$ . Thus, as illustrated in Figure 7, a decrease in  $\beta$  causes the region bounded by the thick curve to contract, while an increase in  $\beta$  causes this region to expand. One implication is that, starting from the case in the upper panel where  $\beta = .1$ , an increase in  $\beta$  would cause the thick curve to shift rightward in the neighborhood of ( $r = .009, \sigma_F = .046$ ), and the equilibrium growth rate would increase.

The existence of multiple equilibria raises the possibility of catastrophes. That is, a small (continuous) change in a parameter value might cause an abrupt (discontinuous) change in the equilibrium outcome. In particular, we might consider whether a small decrease in the fertility rate could cause a discontinuous jump downward in the equilibrium growth rate. For the preceding example, Figure 7 reveals that a gradual decrease in the fertility rate from  $\beta = .1$  to  $\beta = .08$  would cause the equilibrium growth rate to fall smoothly from  $r^* = .009$  to  $r^* = .001$ . Further gradual decreases in  $\beta$  would continue to shift the thick curve slowly leftward, and simulation analysis reveals that equilibria along the lower arm of the thin curve are stable. One can show that, as the fertility rate gradually decreases to  $\beta = .06$  and  $\beta = .04$ , the equilibrium growth rates would fall smoothly to  $r^* = -.005$  (with  $\sigma_F^* = .031$ ) and  $r^* = -.018$  (with  $\sigma_F^* = .013$ ). Thus, for the scenario just described, a gradual decrease in the fertility rate would not cause any catastrophic change in the equilibrium growth rate.

However, as illustrated in Figure 8, this sort of catastrophe can arise given other parameter values. Given  $\beta = .07$ , the top panel indicates five different equilibria: ( $r^* = .001, \sigma_F^* = .046$ ), a pair of mirror-image equilibria ( $r^* = -.005, \sigma_F^* = .080$ ) and ( $r^* = -.005, \sigma_F^* = .023$ ), and another pair of mirror-image equilibria ( $r^* = -.089, \sigma_F^* = .075$ ) and ( $r^* = -.089, \sigma_F^* = .001$ ). Simulation analysis reveals that the equilibria with highest and lowest growth rates are stable, while the equilibria with the intermediate growth rate are unstable. Given  $\beta = .06$ , the bottom panel

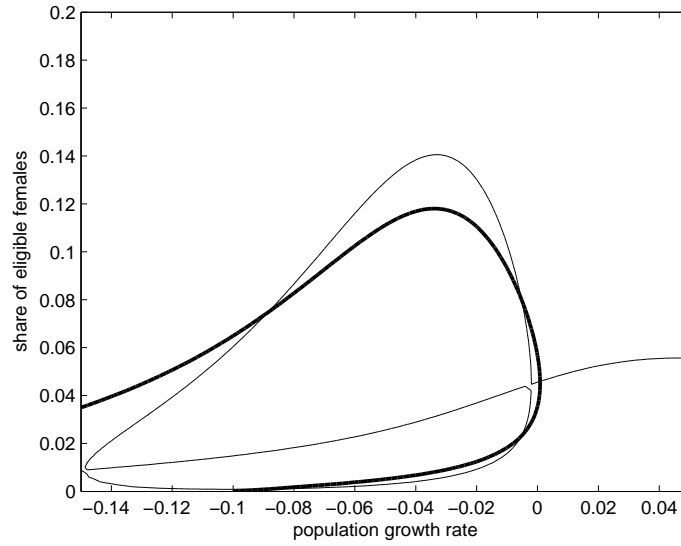
**Figure 7: Endogenous growth equilibria**



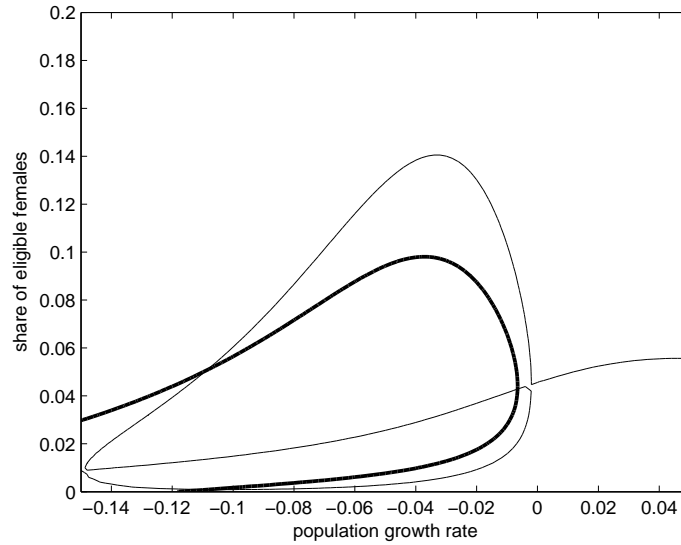
*These diagrams assume  $\mu = 3$ ,  $s = 1$ ,  $\alpha_F = \alpha_M = 20$ ,  $\gamma_F = \gamma_M = 60$ ,  $\omega_F = \omega_M = 80$ ,  $H = 1/h = 10$ ,  $\kappa_F = 40$ , and  $\kappa_M = 60$ . The fertility rate  $\beta$  varies across diagrams as indicated. The thin curves indicate solutions to equation (37); the thick curves indicate solutions to equation (51). Equilibria  $(r^*, \sigma_F^*)$  correspond to the intersections of these curves.*

**Figure 8: A catastrophe**

$$\beta = .07$$



$$\beta = .06$$



*These diagrams assume  $\mu = 3$ ,  $s = 1$ ,  $\alpha_F = \alpha_M = 15$ ,  $\gamma_F = \gamma_M = 60$ ,  $\omega_F = \omega_M = 80$ ,  $H = 1/h = 10$ , and  $\kappa_F = \kappa_M = 40$ . The fertility rate  $\beta$  varies across diagrams as indicated. The thin curves indicate solutions to equation (37); the thick curves indicate solutions to equation (51). Equilibria  $(r^*, \sigma_F^*)$  correspond to the intersections of these curves.*

indicates three different equilibria: ( $r^* = -.006, \sigma_F^* = .043$ ), and a pair of mirror-image equilibria ( $r^* = -.109, \sigma_F^* = .051$ ) and ( $r^* = -.109, \sigma_F^* = .001$ ). Simulation analysis reveals that the equilibrium with the higher growth rate is unstable, while the equilibria with lower growth rates are stable.

The instability of the equilibrium with  $r^* = -.006$  for  $\beta = .06$  creates the potential for a catastrophe. Suppose the fertility rate is  $\beta = .07$  and the population is initially in the positive growth equilibrium. If the fertility rate decreases slightly to  $\beta = .06$ , the population moves from ( $r = .001, \sigma_F = .046$ ) toward the equilibrium ( $r^* = -.006, \sigma_F^* = .043$ ). However, because this equilibrium is not stable, the population will diverge (slowly at first) from this outcome. In the process, the growth rate will continue to fall until the population ultimately reaches one of the stable equilibria. Thus, given a small change in the fertility rate from from .07 to .06, the equilibrium growth rate jumps discontinuously downward from 0% to nearly  $-11\%$ .

Equations (37) and (51) determine existence but not stability of equilibria, and it is important to recognize the high dimensionality of the dynamical system composed of equations (5-13). Nevertheless, a naive interpretation of Figures 7 and 8 as phase diagrams for a two-dimensional dynamical system does provide some insight into disequilibrium dynamics. On this interpretation,

$$\text{sign}\{d\sigma_F/dt\} = \text{sign}\{\chi_F(\chi_M(\sigma_F)) - \sigma_F\} \quad (53)$$

$$\text{sign}\{dr/dt\} = \text{sign}\{\rho(r, \sigma_F, \chi_M(\sigma_F)) - (1 + hr)\} \quad (54)$$

To illustrate, consider again Figure 8. For the top panel ( $\beta = .07$ ), these dynamics suggest stability of the equilibrium ( $r^* = .001, \sigma_F^* = .046$ ). Within the neighborhood of this equilibrium, both  $r$  and  $\sigma_F$  would converge to the equilibrium levels. In contrast, for the bottom panel ( $\beta = .06$ ), these dynamics suggest instability of the equilibrium ( $r^* = -.006, \sigma_F^* = .043$ ). Within the neighborhood of this equilibrium,  $r$  would converge to the equilibrium, but  $\sigma_F$  would diverge. Consistent with this naive phase-diagram analysis, simulations reveal that the population initially diverges by following a path along the thick black curve away from the unstable equilibrium.

However, these “phase diagrams” may be a poor guide to disequilibrium dynamics in other cases, especially given the potential for limit cycles.<sup>7</sup> Figure 9 illustrates. In the top panel,  $\chi_F(\chi_M(\sigma_F)) - \sigma_F$  is negative above the thin curve and positive below it, while  $\rho(r, \sigma_F, \chi_M(\sigma_F)) - (1 + hr)$  is positive to the left of the thick curve and negative to the right. Equations (53-54) would thus suggest convergence of the population to the equilibrium ( $r^* = .028, \sigma_F^* = .106$ ). But simulation analysis reveals the population actually converges to the limit cycle indicated by the dotted curve in the top panel and the time paths in the bottom panel.

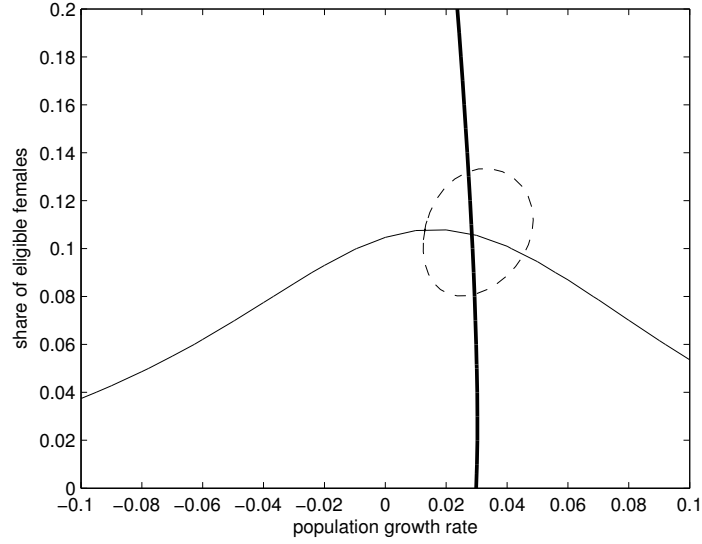
Further examples suggest that limit cycles arise only when the reproductive age ranges are relatively short. That is, fixing the earliest ages at which individuals reproduce ( $\alpha_F$  and  $\alpha_M$ ), limit cycles arise only when the final ages ( $\kappa_F$  and  $\kappa_M$ ) are

---

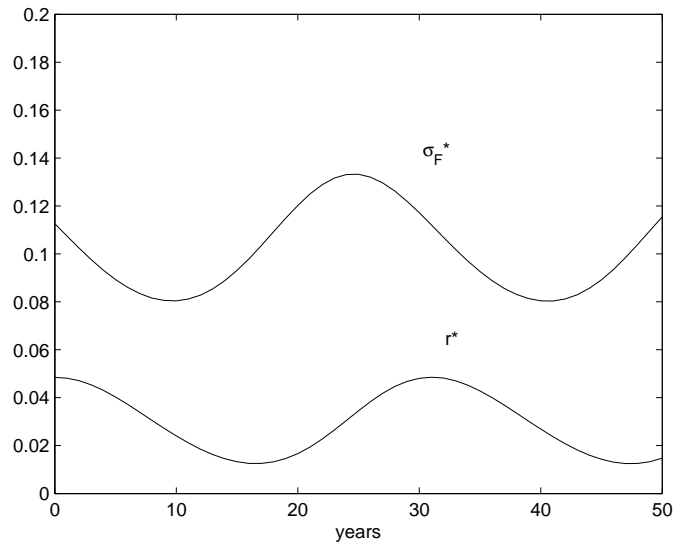
<sup>7</sup>See Caswell and Weeks (1986) for a discussion of limit cycles in two-sex models.

Figure 9: A limit cycle

Orbit diagram



Time paths



This example assumes  $\mu = .5$ ,  $s = 1$ ,  $\alpha_F = \alpha_M = 20$ ,  $\gamma_F = \gamma_M = 60$ ,  $\omega_F = \omega_M = 80$ ,  $H = 1/h = 10$ ,  $\kappa_F = \kappa_M = 40$ , and  $\beta = .5$ . In the top panel, the thin curve indicates solutions to equation (37), the thick curve indicates solutions to equation (51), and the dotted curve indicates the limit cycle revealed by simulation analysis. The bottom panel shows the time path of the growth rate  $r$  and the share of eligible females  $\sigma_F$  after population dynamics have converged to the limit cycle.

relatively low. To illustrate, Figure 10 varies these parameters while holding fixed the other parameters from Figure 9. The dotted curves on the upper-left diagrams indicate that the population converges to a limit cycles, while the absence of dotted curves in the other diagrams indicates that the population converges to the steady state determined by the intersection of the thin and thick curves.

## 5 Conclusion

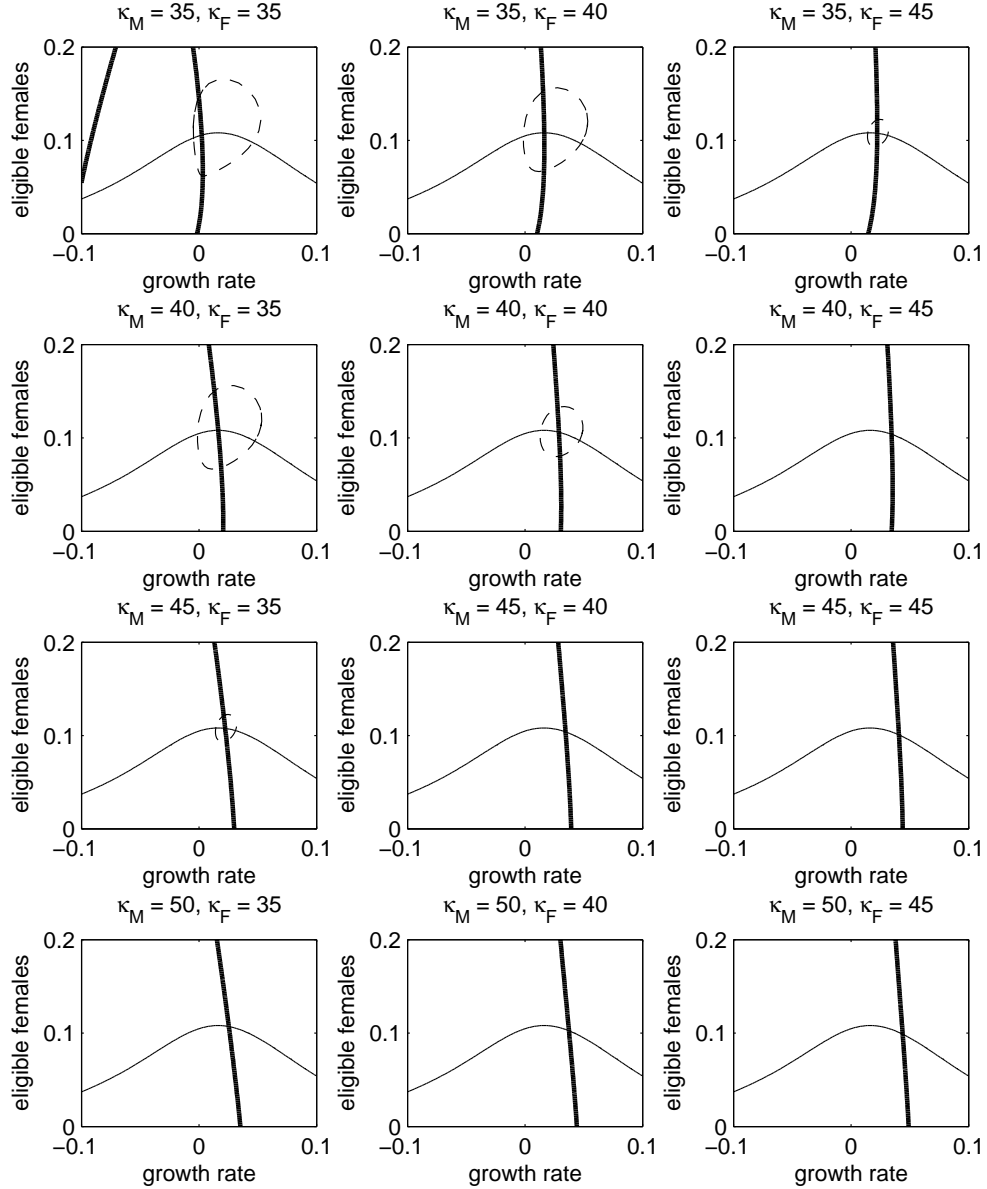
This paper examines an age-structured two-sex model in which couples dissolve only through the death of a spouse, and widows never remarry. Additional simplifying assumptions on the matching function (individuals meet through random mixing of the population; eligible singles have no age preference over potential partners) yield a highly tractable model. In the exogenous-growth version, an equilibrium is fully characterized by a single variable (the share of eligible females in the population). In the endogenous-growth version, an equilibrium is characterized by a pair of variables (the growth rate as well as the share of eligible females). In both versions, equilibria can be determined through simple graphical methods.

While other age-structured two-sex models are more general and more realistic, their complexity has precluded analysis of the stability and uniqueness of equilibria. In contrast, the tractability of the present model permits some new insight into conditions under which multiple equilibria arise. In the exogenous-growth model, we prove that multiple equilibria arise only if the growth rate is negative. Numerical examples further indicate that multiplicity requires either a high matching rate or a large range of eligible ages. In the endogenous-growth model, numerical examples demonstrate the potential for multiple equilibria, catastrophes, and limit cycles.

Though the practical importance of these results is somewhat difficult to judge without generalization of the model and calibration of model parameters, our findings might suggest that multiple equilibria are not likely to arise in realistic settings given the ranges of parameter values that would be associated with observed human populations. In particular, while our leading examples (Figures 1 to 4) assumed a very large range of eligible ages (20 to 60 years), we might expect this range to be smaller in observed populations (at least under the maintained assumption that eligible singles are indifferent to the age of potential partners). Further, intuition suggests that divorce and remarriage, by increasing the availability of eligible singles at older ages, might further limit the potential for multiple equilibria.

On the other hand, we note that the exogenous-growth version of our model is similar to the MSQUEEZ model developed by Schoen (1983). In parallel to our analysis, Schoen derived the equilibrium population structure for exogenous growth rates between  $-20\%$  and  $+20\%$ . But in contrast to our analysis, the iterative procedure he used to compute these equilibria would not have detected the existence of multi-

Figure 10: Equilibrium outcomes by  $\kappa_M$  and  $\kappa_F$



The parameter values  $\mu = .5$ ,  $s = 1$ ,  $\alpha_F = \alpha_M = 20$ ,  $\gamma_F = \gamma_M = 60$ ,  $\omega_F = \omega_M = 80$ ,  $H = 1/h = 5$ , and  $\beta = .5$  are fixed across all diagrams. The parameters  $\kappa_F$  and  $\kappa_M$  vary across the diagrams as indicated. Following the format of the top panel of Figure 9, the dotted lines indicate limit cycles revealed by simulation analysis. For the diagrams without dotted lines, the population converges to the steady state indicated by the intersection of the thin and thick curves.

ple equilibria.<sup>8</sup> Perhaps there was no potential for multiple equilibria given Schoen’s (harmonic mean) specification of the matching function or his (empirically grounded) specification of matching parameters. But our present results might encourage future researchers to consider this possibility.

Our finding that multiple equilibria arise in the exogenous-growth model only if the growth rate is negative might seem to further limit the practical relevance of our results. Obviously, populations with negative growth rates will ultimately become extinct. However, our examples indicate that multiple equilibria can arise even when the growth rate is only slightly negative. While speculative, our findings might encourage researchers to explore the theoretical potential for multiple equilibria or even catastrophic change in countries currently experiencing negative growth or below-replacement fertility.

The tractability of the present model allows equilibria to be determined through a two-equation system that can be analyzed graphically. Future theoretical work might see how far the model can be generalized without losing this attractive implication. While tractability hinges on the two simplifying assumptions on the matching function, other simplifying assumptions were made merely for convenience. In particular, it would be straightforward to allow arbitrary patterns of mortality ( $\delta_F$  and  $\delta_M$  varying by the individual’s age) or fertility ( $\beta$  varying by the ages of partners). Potentially, the model could also be extended to allow divorce and remarriage without moving beyond our two-equation framework, since the distribution of couples would still be determined by the distributions of singles, though the form of the dependence would become more complicated.

While motivated by tractability considerations, our key assumptions on the matching function might be defended on substantive grounds. In the absence of consensus on the best specification of the matching function (Pollard 1997, Ianelli et al 2005), random mixing provides a useful baseline. Age preference among eligible singles may be weaker than generally assumed (Bhrolcháin 2001), and we have shown that strong positive sorting by age can arise solely through availability considerations (recall the lower panel of Figure 2). Nevertheless, empirical realism surely warrants more general specifications of the matching function. We hope that the present paper, by beginning to identify the conditions under which multiple equilibria arise, will prove useful as researchers continue to grapple with more general (and harder to analyze) age-structured two-sex models.

---

<sup>8</sup>In that procedure, initial conditions were taken from empirical one-sex life tables. A wider range of initial conditions would be needed to address the existence (or non-existence) of multiple equilibria.

## 6 Appendix

In this appendix, we prove that multiple equilibria arise in the exogeneous-growth model only if the growth rate is negative.

The continuous-time analogs of equations (33) and (34) are

$$\chi_F(\sigma_M) = \frac{1}{N} e^{-\alpha_F r} \int_0^{\gamma_F - \alpha_F} e^{-(r + \mu \sigma_M)i} \mathrm{d}i \quad (55)$$

$$\chi_M(\sigma_F) = \frac{1}{N} s e^{-\alpha_M r} \int_0^{\gamma_M - \alpha_M} e^{-(r + \mu \sigma_F)j} \mathrm{d}j \quad (56)$$

and hence the derivatives are

$$\chi_F'(\sigma_M) = -\mu \frac{1}{N} e^{-\alpha_F r} \int_0^{\gamma_F - \alpha_F} i e^{-(r + \mu \sigma_M)i} \mathrm{d}i \quad (57)$$

$$\chi_M'(\sigma_F) = -\mu \frac{1}{N} s e^{-\alpha_M r} \int_0^{\gamma_M - \alpha_M} j e^{-(r + \mu \sigma_F)j} \mathrm{d}j \quad (58)$$

The slope of the compound function  $\chi_F(\chi_M(\sigma_F))$  can be written

$$\chi_F'(\chi_M(\sigma_F)) \cdot \chi_M'(\sigma_F) \quad (59)$$

which, evaluated at the fixed point  $\sigma_F^*$ , becomes

$$\chi_F'(\sigma_M^*) \cdot \chi_M'(\sigma_F^*) \quad (60)$$

Using equation (36), this product may be rewritten as

$$\frac{\sigma_M^* \chi_F'(\sigma_M^*)}{\chi_F(\sigma_M^*)} \cdot \frac{\sigma_F^* \chi_M'(\sigma_F^*)}{\chi_M(\sigma_F^*)} \quad (61)$$

which is equal to

$$\frac{\sigma_M^* \mu \int_0^{\gamma_F - \alpha_F} i e^{-(r + \mu \sigma_M^*)i} \mathrm{d}i}{\int_0^{\gamma_F - \alpha_F} e^{-(r + \mu \sigma_M^*)i} \mathrm{d}i} \cdot \frac{\sigma_F^* \mu \int_0^{\gamma_M - \alpha_M} j e^{-(r + \mu \sigma_F^*)j} \mathrm{d}j}{\int_0^{\gamma_M - \alpha_M} e^{-(r + \mu \sigma_F^*)j} \mathrm{d}j} \quad (62)$$

Note that both terms in equation (62) take the form

$$\zeta(r) = \frac{x \int_0^b i e^{-(r+x)i} \mathrm{d}i}{\int_0^b e^{-(r+x)i} \mathrm{d}i} \quad (63)$$

where  $\zeta(0) < 1$  for  $b < \infty$ , and  $\zeta'(r) < 0$ . Thus, when the growth rate  $r$  is non-negative, both terms in equation (62) are less than 1. Consequently, the slope of the compound function  $\chi_F(\chi_M(\sigma_F))$  must be less than 1 at any fixed point  $\sigma_F^*$ . Recalling that the compound function is continuous and increasing and satisfies equation (38), this guarantees the existence of a unique fixed point.

## References

- Allman, Elizabeth S. and John A. Rhodes (2004) *Mathematical Models in Biology: An Introduction*. New York: Cambridge University Press.
- Bhrolcháin, Maire Ni (2001) “Flexibility in the Marriage Market,” *Population: An English Selection* 13:9-47.
- Caswell, H and D E Weeks (1986) “Two-Sex Models: Chaos, Extinction, and Other Dynamic Consequences of Sex,” *American Naturalist* 128:707-735.
- Guilmoto, Christophe Z (2012) “Skewed Sex Ratios at Birth and Future Marriage Squeeze in China and India, 2005-2100,” *Demography* 49:77-100.
- Hadeler, K P (1989) “Pair Formation in Age-Structured Populations,” *Acta Applicandae Mathematicae* 14:91-102.
- (1993) “Pair Formation Models with Maturation Period,” *Journal of Mathematical Biology* 32:1-15.
- Hoppensteadt, Frank (1975) *Mathematical Theories of Populations: Demographics, Genetics and Epidemics*. Philadelphia: SIAM.
- Iannelli, M, M Martcheva, and F A Milner (2005) *Gender-Structured Population Modeling: Mathematical Methods, Numerics, and Simulations*. Philadelphia: SIAM.
- Inaba, Hisashi (1993) “An Age-Structured Two-Sex Model for Human Population Reproduction by First Marriage,” Working Paper Series No. 15, Institute of Population Problems, Ministry of Health and Welfare, Japan.
- (2000) “Persistent Age Distributions for an Age-Structured Two-Sex Population Model,” *Mathematical Population Studies* 7:365-398.
- Keyfitz, Nathan (1972) “The Mathematics of Sex and Marriage” in *Proceedings of the Sixth Berkeley Symposium on Mathematical Statistics and Probability*, Vol 4. Berkeley: University of California Press.
- Martcheva, Maia (1999) “Exponential Growth in Age-Structured Two-Sex Populations,” *Mathematical Biosciences* 157:1-22.

- Pollak, Robert A (1986) "A Reformulation of the Two-Sex Problem," *Demography* 23:247-259.
- (1990) "Two-Sex Demographic Models," *Journal of Political Economy* 98:399-420.
- Pollard, J H (1997) "Modelling the Interaction Between the Sexes," *Mathematical and Computational Modeling* 26:11-24.
- Prüss, Jan and Wilhelm Schappacher (1993) "Persistent Age Distributions for a Pair-Formation Model," *Journal of Mathematical Biology* 33:17-33.
- Schoen, Robert (1983) "Measuring the Tightness of a Marriage Squeeze," *Demography* 20:61-78.
- (1988) *Modeling Multigroup Populations*. New York: Plenum Press.